INTERFEROMETRIC STUDY OF HEAT TRANSFER IN A GROOVED GEOMETRY

C. V. Herman, F. Mayinger

Lehrstuhl A für Thermodynamik, TU München
Arcisstraße 21, 8000 München 2, FRG.

ABSTRACT

The paper treats heat transfer in a grooved geometry with flow direction perpendicular to the direction of the propagation of the grooves. In laminar flow conditions the thermal boundary layer develops along the test section, a parallel plate duct with one plane wall at ambient temperature and one heated grooved wall. The aspect ratio of the grooves is width (w) : depth (h) = 4 : 1 and the ratio of channel width (2h) : groove depth (h) = 2 : 1. In order to obtain data on the temperature fields in this complex geometry without disturbing the physical situation, the experimental method of holographic interferometry was selected. From the visualized temperature fields, temperature profiles were reconstructed and heat transfer data was evaluated. The heat transfer process is discussed in detail, based on results obtained for three different Reynolds numbers.

INTRODUCTION

In order to improve the thermal performance of heat transfer devices, methods and possibilities of heat transfer augmentation are being investigated [1]. One of the possibilities is the modification of the basic geometry, in our case a parallel plate duct, by introducing transversal grooves, in order to periodically interrupt the plane heat transfer surface, thus causing flow separation and a periodical redevelopment of the thermal boundary layer characterized by high heat transfer coefficients.

The physical situation considered in the paper (grooved geometry, figure 1) is encountered in numerous engineering applications: cooling of reactor cores, biomedical applications, design of heat exchangers, cooling of electronic equipment and so on. In practical applications both the developing and the fully developed flow situation is of interest. Problems of heat transfer in the basic geometry — parallel plate ducts and rectangular ducts — were reviewed and treated in detail in the literature [2]. Of practical interest is the experimental work of Aung (1983) [3], who analysed heat transfer on a single cavity and the influence of the aspect ratio of the cavity on heat transfer by means of interferometry. Heat transfer and fluid flow in a periodically

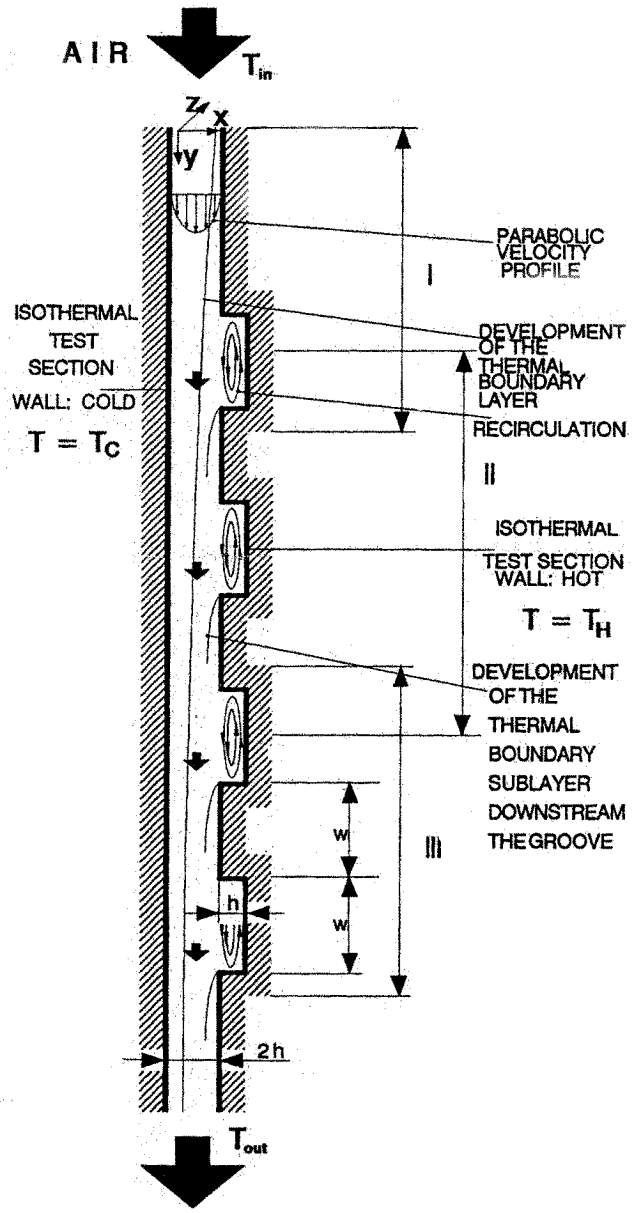

Fig. 1 Schematic of the investigated geometry and the physical situation

Experimental Heat Transfer, Fluid Mechanics, and Thermodynamics 1991
J.F. Keffer, R.K. Shah, and E.N. Ganić, Editors

grooved geometry for fully developed flow and periodically repeating thermal conditions was treated in [4], [5], [6]. Especially possibilities of resonant heat transfer enhancement were analysed, and the experimental results confirmed the numerical predictions [7]. Two dimensional channel flow over two fences in tandem was investigated experimentally by means of laser- Doppler anemometry and also numerically in [8]. Trollheden and Sundén (1987) [9] numerically investigated laminar flow in a parallel plate channel with large cavities, a geometry similar to the one treated in this paper. The duct walls were held at constant temperature (heated symmetrically) and the flow field was fully developed with periodically repeating cycles. Thermally fully developed regime was present — contrasted to the thermally developing situation analysed in this paper. They have found that moderate heat transfer augmentation was achieved with high pressure drop penalty in comparison to values for a straight duct. In [10] Sundén and Trollheden investigated the same geometry with uniform heat flux imposed at the channel walls, and found a decrease in heat transfer compared to the corrugated channel. Hunter and Collins (1987) [11] used holographic interferometry to visualize and reconstruct three dimensional instationary temperature fields and they investigated heat transfer in turbulent flow on a single flat plate and on ribbed geometries. Fodemski and Collins (1988) [12] used numerical simulation to study heat transfer and fluid flow over a transversely ribbed surface in a rectangular channel. Their results showed very good agreement with the experimental results obtained by interferometry [11].

The geometry treated in this paper is presented schematically in figure 1, and it stands as model for the cooling of electronic circuit boards with grooves representing regions between electronic components. Heat transfer is analysed experimentally (some results of the investigation are presented in [13]) in a parallel plate channel with four transversal grooves on the heated wall. The grooves and the channel regions between the grooves are w = 0.02 m long, the depth of the grooves is h = 0.005 m, corresponding to one half of the channel height. Thermal boundary conditions are given by isothermal test section walls (T_H hot wall, T_C - cold wall) and the flow is fully developed with parabolic velocity profiles at the entrance of the test section. The thermal boundary layer develops along the heated wall of the test section and the influence of the grooves on the heat transfer process is investigated. The improvement of heat transfer is accompanied by increased pressure drops. The two-dimensional temperature fields were visualized and reconstructed using holographic interferometry in the laminar flow regime.

THE EXPERIMENTAL ARRANGEMENT

The experimental arrangement used in the heat transfer measurements and in the visualization of temperature fields is presented schematically in figure 2. The experimental channel is in vertical position and it consists of the entry

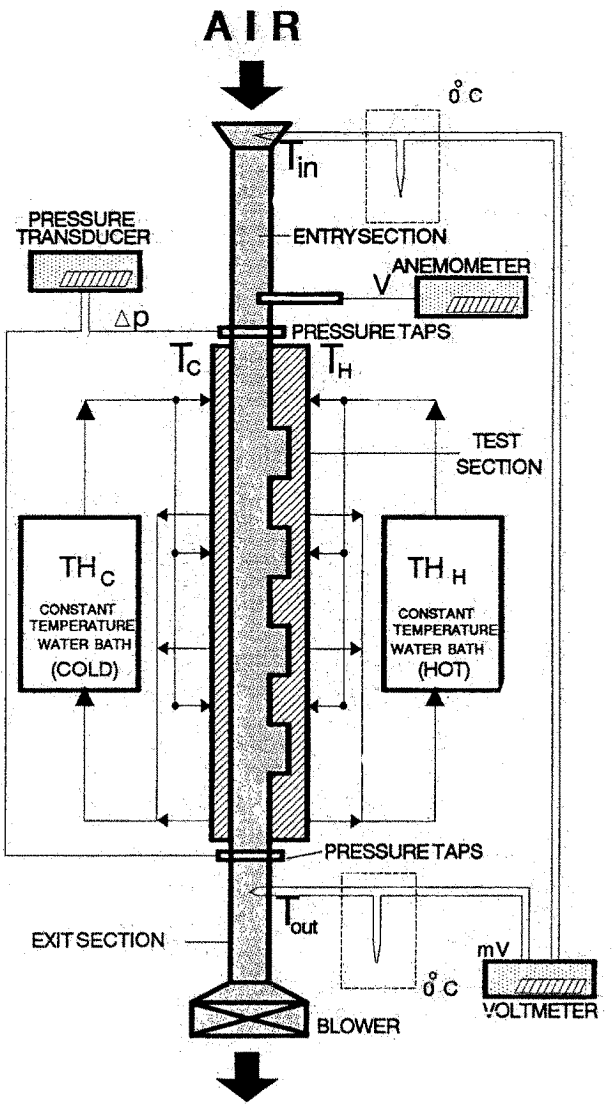

Figure 2. Schematic of the experimental setup

section, the test section and the exit section. The entry section is 0.9 m long (y direction), 2h = 0.01 m high (x direction) and d = 0.22 m wide (z direction, corresponds to the direction and length of transillumination by laser light) parallel plate duct. The test section is 0.22 m long and both its walls, manufactured of aluminium, are provided with water channels. Circulating water from two constant temperature water baths (TH_H for the hot wall and TH_C the cold wall), in three parallel loops for each channel wall, keeps wall temperatures constant to provide good isothermal boundary conditions. A temperature difference is maintained between the test section walls by keeping the plane cold wall at ambient temperature and by heating the grooved wall. The front and back walls of the test section are of glass to enable the transillumination of the investigated region. The exit section, 0.3 m long, carries the blower creating the air flow. The direction of the flow is indicated

by arrows in figures 1 and 2. The blower is operating in a suction mode, and the flow velocity is varied by varying the dc supply voltage.

Air inlet and outlet temperatures were measured by two batteries of nickelchrom-constantan thermocouples at locations indicated in figure 2. Flow velocity profile measurements were taken by a Schiltknecht hot wire anemometer thermo air type 442 calibrated by a rotameter. In the pressure drop measurements, a pressure transducer Setra Series 239 calibrated by a Betz manometer was used. The pressure transducer was connected to the four pressure taps, 0.0001 m in diameter, located in the flange between the entry and test section and in the flange between the test section and the exit section. The temperatures of the hot wall and of the cold wall were measured by 25 nickelchrom-constantan thermocouples with junctions at the wall surface and they provided reference values for the interferometric measurements.

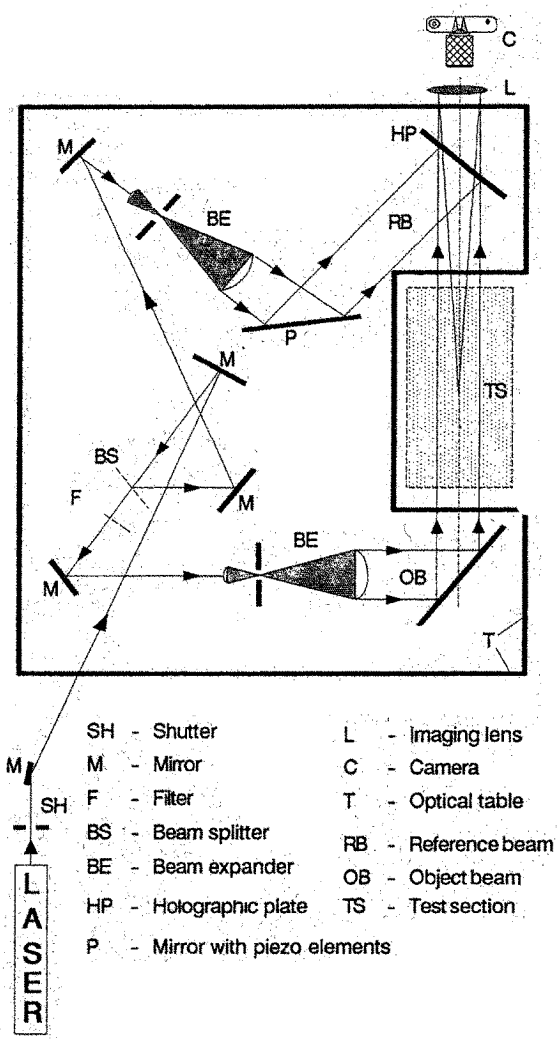

Fig. 3 Schematic of the optical arrangement for holographic interferometry used in the investigation of heat transfer in the grooved geometry

THE EXPERIMENTAL METHOD

Holographic interferometry is an experimental method widely applied in the study of transport phenomena ([14], [15], [16]) and it was used in the visualization of temperature fields in the experiments described in this paper. Thus qualitative information on the temperature fields and — by evaluating interferograms — also quantitative heat transfer data was obtained without disturbing the investigated physical process.

The optical setup used in the measurements is presented schematically in figure 3. It corresponds to the basic optical arrangement discussed in [14], [15] and it will not be treated here. Details on reconstruction of temperature profiles from interferograms are given in [17]. An Argon ionen laser with $\lambda = 514.5$ nm wavelength and 0.5 m coherence length was used as light source. The measurements were obtained by the real time method: the reference state (test section at ambient temperature) was first recorded on the holographic plate which was afterwards processed and accurately repositioned into its original position. Then the investigated physical process was started; the test section walls were brought to the desired temperatures and flow velocities were varied. Interferograms were recorded on photographic film, and the processed negatives were then analysed and measured by a photometer.

As the test section is longer (0.22 m) than the diameter of the expanded laser beam (0.078 m), temperature fields were recorded at three different heights of the test section (marked by I, II and III in figure 1).

RESULTS AND DISCUSSION

Eperimental Parameters

The thermal boundary conditions in heat transfer measurements in the grooved geometry are isothermal test section walls (T_H for the heated wall and T_C for the plane wall at T_{in}) (realized with an accuracy of 0.5 K). The average temperature difference between hot and cold wall $\overline{\Delta T}$ was evaluated by taking average values of thermocouple readings and it was kept constant in the visualization experiments at different test section heights.

Flow velocity measurements have prooved that fully developed flow conditions with approximately parabolic velocity profiles were present at the entrance of the test section. Experimental runs were performed for Reynolds numbers in the range from Re = 290 to Re = 2000. The Reynolds number was defined with the hydraulic diameter D_h ($D_h = 4\ (2h\ d)\ /\ 2\ (2h + d)$) as the characteristic length,

$$\mathrm{Re} = v_m D_h / \nu. \qquad (1)$$

Experimental Uncertainity

Flow velocities were measured at three cross sections of the channel using hot wire anemometer calibrated by a rotameter. From the measured velocity profiles, the cross channel average flow velocity v_m was evaluated with an

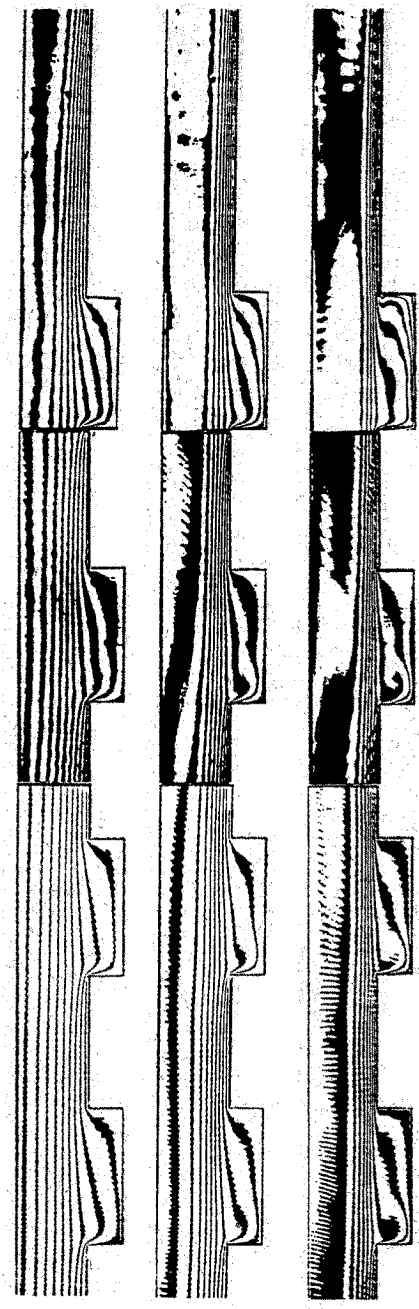

Fig. 4 Typical interferogram sets for Re = 293, Re = 604 and Re = 1561 taken by the infinite fringe field arrangement. The average temperature difference between the hot and the cold wall is $\overline{\Delta T}$ = 30 K. Fringes correspond to isotherms with ΔT/fringe pair ≈ 3 K.

estimated accuracy of 7%. In the reconstruction of *temperature profiles* from interferometric images a case study has shown that the influence of the viewing windows contributes most significantly to this error, smaller are the contributions of the uncertainities in the determination of the locations of fringe extrema and the misalignment of the test section and the expanded laser beam. The effects of uncertainities in the determination of the wall positions were negligible. Calculations have shown that the parabolic approximation [17] provides sufficient accuracy in the reconstruction of temperature profiles for the temperature gradients present in these measurements. The temperature values obtained from interferometric measurements were compared with thermocouple readings and the errors connected to the evaluation of temperature profiles were estimated to 7%. More details about the error analysis can be found in [18]. The local *Nusselt numbers* were evaluated from the temperature gradient on the heated wall with an estimated accuracy of 8.5%. These results were compared with direct temperature gradient measurements from finite fringe alignment interferograms [15] and showed good agreement. Errors in pressure drop measurements were estimated to 6%.

Temperature fields

A set of interferograms for $\overline{\Delta T}$ = 30 K and three different Reynolds numbers obtained by using the infinite fringe field technique is presented in figure 4, and is representative of the thermal behaviour of the system [13]. In the pictures, the three segments at the different heights of the test section (I, II, III, figure 1) are clearly recognizable and the temperature fields show very good agreement. Interferograms were evaluated by measuring locations of fringe minima and maxima at different cross sections of the test channel using a photometer.

In figure 4, two main heat transfer regions can be recognized: (i) the main channel region and (ii) the groove region. In the groove region temperature profiles are under the influence of the recirculating flow. No significant influence of recirculation in the channel part of the flow can be observed, and the temperature drop in this region is relatively high compared to the temperture drop in the groove (also obvious from figures 5 and 6). The thickness of the developing thermal boundary layer along the test section decreases with increasing Reynolds number and the temperature gradients at the heated channel wall also increase with higher values of Reynolds numbers — similarly to the situation in thermally developing duct flow with asymmetrical heating. A gradual decrease of the temperature gradient along the test section in the channel region is observable. The visualized temperature fields agree qualitatively with the results obtained by numerical simulation [4], [5], [9], [11].

Figures 5 and 6 show temperature profiles evaluated from the interferograms for Re = 1481 and an average temperature difference $\overline{\Delta T}$ = 43.0 K for characteristic channel cross sections in the groove region and in the main channel region. The evaluated temperatures were scaled by $\overline{\Delta T}$ in order to obtain comparable results for the different experimental runs by different values of $T_C = T_{in}$ in the three channel heights. In figure 5, temperature profiles at four different cross sections in the region of the first groove are presented. The temperature profiles show a characteristic S shape. The temperature gradient at the heated wall is

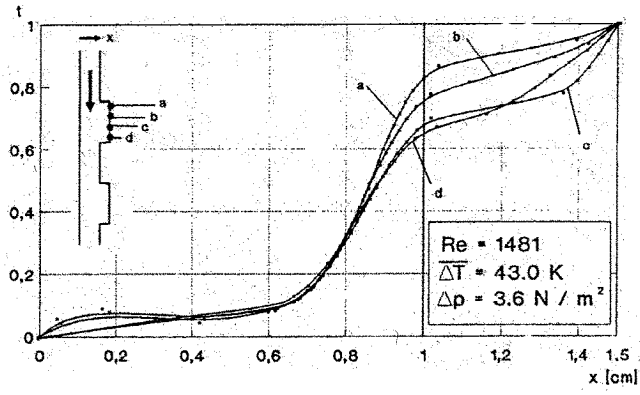

Fig. 5 Typical reconstructed temperature profiles ($t = (T(x) - T_C) / (T_H - T_C)$) at cross sections a) y = 5.36 cm, b) y = 5.89 cm, c) y = 6.66 cm and d) y = 6.87 cm in the region of the first groove for Re = 1481 and $\overline{\Delta T}$ = 43 K.

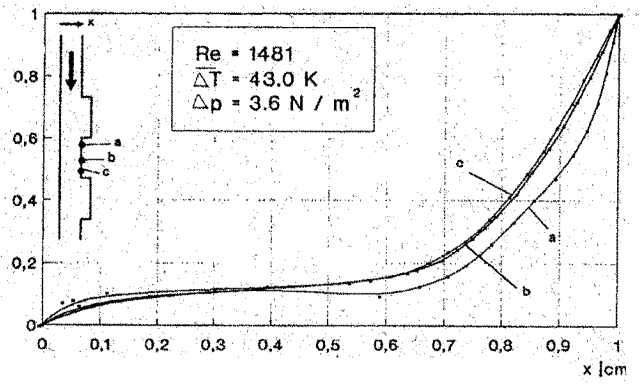

Fig. 6 Typical reconstructed temperature pronles ($t = (T(x) - T_C) / (T_H - T_C)$) at cross sections a) y = 7.16 cm, b) y = 8.40 cm and c) y = 8.89 cm between the first groove and the second groove for Re = 1481 and $\overline{\Delta T}$ = 43 K.

small near the beginning of the groove, it increases along the groove to reach a maximum in the last quarter section of the groove, and then it decreases towards the closing wall of the groove. Figure 6 shows temperature profiles in the region between the first and the second grooves, in the zone of the redeveloping thermal boundary sublayer. The temperature gradient is high immediately behind the first groove and it gradually decreases towards the second groove.

In figure 7, the temperature fields in the test section as function of the x and the y coordinate are presented for Re = 1481 and $\overline{\Delta T}$ = 43 K .

Local Nusselt Numbers

In figures 8, 9 and 10, local Nusselt numbers Nu(y) along the heated wall (only on the vertical sections) for Re = 620, Re = 1076 and Re = 1481 are presented. The local Nusselt number is evaluated as

$$Nu(y) = \frac{(dT/dx)_w \; D_h}{(T_w - T_\infty)} \qquad (2)$$

In this equation $(dT/dx)_w$ is the temperature gradient at the grooved wall and the bulk temperature T_b (evaluated as $T_b = (T_{in} + T_{out}) / 2$) was taken as reference temperature T_∞. As the temperature of the cold wall corresponds to the ambient temperature as well as to the temperature of the air streaming along this wall, Nusselt numbers were not evaluated for the cold wall.

For all three flow velocities local Nusselt numbers show the same characteristic behaviour. Immediately at the beginning of the first goove they abruptly fall to a fraction of the attached flow value. Along the groove they increase gradually, reaching a maximum at the last quarter section of the groove. After this peak the value of Nu(y) drops abruptly at y locations near the closing wall. Nu(y) values in the groove are lower than in the channel, due to the low velocities in this region [9]. At y locations in the channel region immediately after the groove, Nu(y) reaches a new peak (region of the redeveloping thermal sublayer) — a multiple of the peak value in the groove region. This peak is followed by a gradual decrease of Nu(y) along the test section towards the next groove. The behaviour of Nu(y) described above repeats along the test section for the following groove/channel sections.

Comparing the diagrams in figures 8, 9 and 10, the absolute values of the peaks both in the grooves and in the inter-groove regions are higher for higher Reynolds numbers. At lower Reynolds numbers a nearly periodical trend is observable, while at Re = 1481, the intensities of the maxima gradually decrease with increasing y coordinate. This behaviour can also be recognized in the interferograms presented in figure 3.

The local Nusselt numbers obtained experimentally, agree well with the results of the numerical investigations of Trollheden and Sundén (1987) [9], which were obtained for slightly different values of the Reynolds number for the thermally fully developed regime.

Overall Nusselt Numbers

Figure 11 shows the overall Nusselt number $\overline{Nu}$ versus the Reynolds number. The overall Nusselt number was

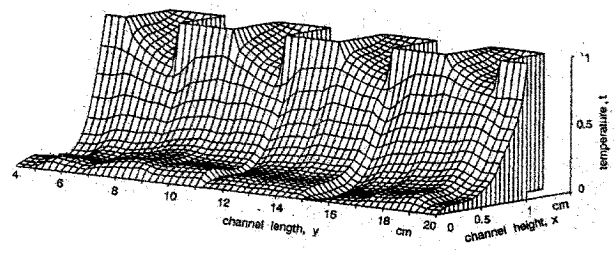

Fig. 7 Temperature fields reconstructed from interferograms at Re = 1481 and $\overline{\Delta T}$ = 43 K.

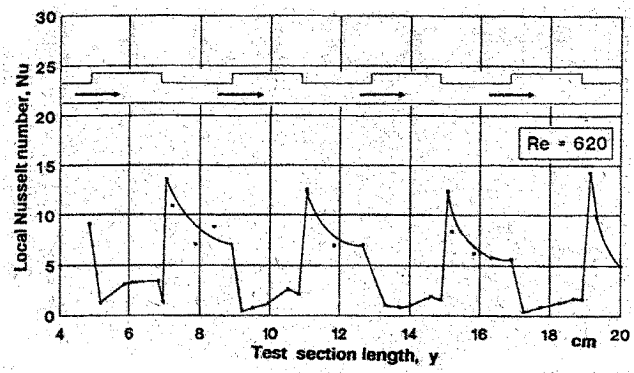

Fig. 8 Local Nusselt number Nu(y) along the test section for Re = 620

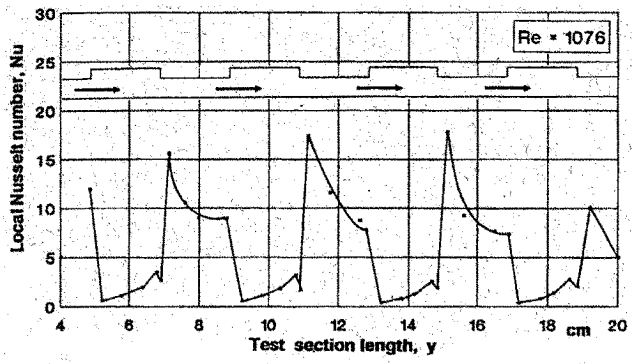

Fig. 9 Local Nusselt number Nu(y) along the test section for Re = 1076

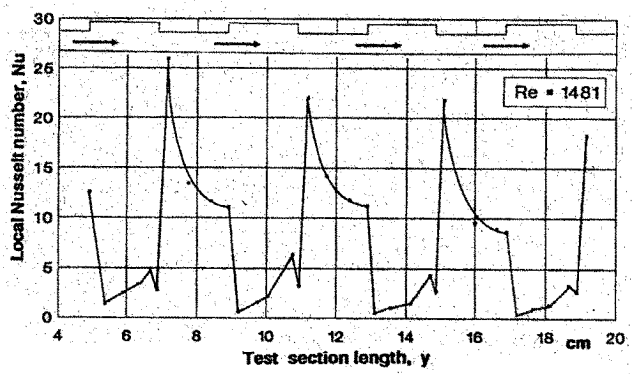

Fig. 10 Local Nusselt number Nu(y) along the test section for Re = 1481

evaluated from the average heat transfer coefficient $\overline{\alpha}_H$ on the grooved wall

$$\overline{Nu} = \frac{\overline{\alpha}_H \, D_h}{k} \qquad (3)$$

with $\overline{\alpha}_H$ as

$$\overline{\alpha}_H = \frac{\dot{m} \, c_p}{A_H} \frac{T_{out} - T_{in}}{T_H - T_b}. \qquad (4)$$

In equation 4, the heat transfer area (hot wall) is denoted with A_H. $\overline{Nu}$ increases monotonuously with the increase of the Reynolds number. The overall Nusselt number for the corresponding basic geometry, a parallel plate duct and fully developed flow, is known [2], $\overline{Nu}_0 = 4$, so that heat transfer enhancement is achieved for regimes with Reynolds numbers above 450.

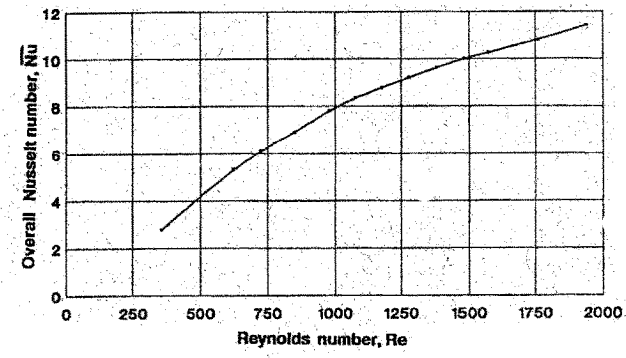

Fig. 11 Overall Nusselt number versus Reynolds number

Outlet-Inlet Temperature Difference

In figure 12, the outlet-inlet temperature difference (T_{out} - T_{in}) scaled by the log mean temperature difference at the grooved wall, evaluated as

$$\Delta T_{m,H} = \frac{(T_H - T_{out}) - (T_H - T_{in})}{\ln\left((T_H - T_{out})/(T_H - T_{in})\right)}, \qquad (5)$$

versus the Reynolds number is presented and it shows a characteristic behaviour. For the lowest Reynolds numbers the difference increases with increasing Reynolds numbers and for flow velocities above Re = 620, the temperature difference decreases.

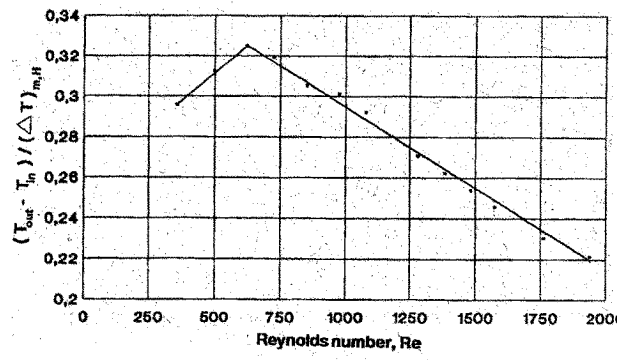

Fig. 12 Overall temperature increase along the test section versus Reynolds number

Pressure drop

Figure 13 shows the measured pressure drop scaled by the calculated values of pressure drop for the basic configuration, fluid flow between parallel flat plates with channel

height 2h and hydrodynamically fully developed conditions, versus the Reynolds number. By introducing grooves into the basic geometry, the pressure drop increases up to a factor of 6.5 for the investigated range of Reynolds numbers. It increases monotonously with increasing Reynolds number.

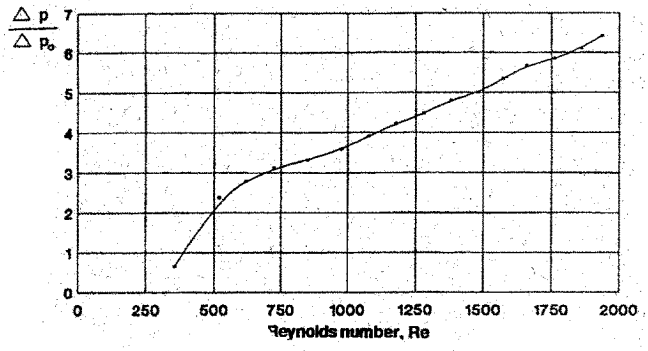

Fig. 13 Pressure drop on the test section Δp scaled by the calculated pressure drop for the basic geometry Δp_0, a parallel plate duct of height 2h, versus Reynolds number.

Practical significance

Grooved geometries are frequently encountered in different cooling applications. In order to improve the performance of heat transfer devices, a good understanding of the physical process is essential. The experimental investigation presented in this paper provides a qualitative insight into the physical phenomenon by visualizing the temperature fields as well as quantitative heat transfer data. A systematic analysis of the influence of groove dimensions and of the length of the region between the grooves on the heat transfer would provide valuable data for design purposes. Future research should be concentrated on the comparison of experimental data and numerical results, in order to obtain sufficient information to predict and eventally optimize system behaviour.

CONCLUSIONS

The experimental results presented in the paper indicate that enhancement of heat transfer in the grooved geometry is achieved, due to the periodical redevelopment of the thermal boundary layer in the region behind the grooves. Heat transfer in the main channel region is essentially uninfluenced by the recirculation in the groove and it contributes the most significant part to the total heat transfer. In the region of the grooves, the heat transfer is under the influence of the recirculating flow, and the temperature gradients at the heated wall are small. Temperature profiles show a characteristic S shape. For higher flow velocities the heat transfer is characterized by higher values of the local Nusselt number along the test section. Increased heat transfer is accompanied by higher pressure drops — compared to the geometry with parallel flat plates — due to the increased skin friction in the redeveloping boundary layer and the existence of recirculating flow regions in the groove.

NOMENCLATURE

- A_H — heat transfer area (hot wall), m^2
- c_p — specific heat at constant pressure, J/kg °C
- d — width of the experimental channel, m
- D_h — hydraulic diameter, m
- h — groove depth and one half of channel height (figure 1), m
- k — thermal conductivity, W/m °C
- $\dot{m}$ — mass rate of flow, kg/s
- Nu — Nusselt number
- $\overline{Nu}$ — overall Nusselt number
- Δp — pressure drop between entry and exit of the test section, N/m^2
- Re — Reynolds number
- t — scaled temperature
- T — temperature, °C
- $\overline{\Delta T}$ — average temperature difference between hot wall and cold wall, K
- v_m — cross channel average flow velocity, m/s
- w — width of the grooves and of the inter-groove region, m
- x — axis of the cartesian coordinate system (figure 1), m
- y — axis of the cartesian coordinate system (figure 1), m
- z — axis of the cartesian coordinate system (figure 1), m
- $\overline{\alpha}_H$ — average heat transfer coefficient (hot wall), W/m^2 °C
- λ — wavelength of laser light, m
- ν — kinematic viscosity, m^2/s

Subscripts

- b — evaluated at bulk conditions
- C — refers to cold wall
- H — refers to hot wall
- in — refers to channel inlet
- out — refers to channel outlet
- w — refers to wall
- 0 — refers to basic geometry (parallel plate duct)
- ∞ — refers to reference value

REFERENCES

1. **Bergles, A. E.**, Techniques to augment heat transfer, in Handbook of heat transfer applications, eds. Rohsenow, W. M., Hartnett, J. P., Ganić, E. N., McGraw-Hill, NY, 1985.
2. **Shah, R. K., London, A. L.**, Laminar flow forced convection in ducts, in Advances in Heat Transfer, T. F. Irvine and J. P. Hartnett eds., Suppl. 1, 1978.

3. **Aung, W.**, An interferometric investigation of separated forced convection in laminar flow past cavities, ASME J. Heat Transfer, Vol. 106, pp. 505-512, 1983.

4. **Ghaddar, N. K., Korczak, K. Z., Mikić, B. B., Patera, A. T.**, Numerical investigation of incompressible flow in grooved channels. Part 1. Stability and self-sustained oscillations, J. Fluid Mech., Vol. 163, pp. 99- 127, 1986.

5. **Ghaddar, N. K., Magen, M., Mikić, B. B., Patera, A. T.**, Numerical investigation of incompressible flow in grooved channels. Part 2. Resonance and oscillatory heat transfer enhancement, J. Fluid Mech., Vol. 168, pp. 541-567, 1986.

6. **Amon, C. H., Mikić, B. B.**, Flow pattern and heat transfer enhancement in self-susteined oscillatory flows, paper AAIA - 89-0428 27th Aerospace Science Meeting, Reno, Nevada, 1989.

7. **Patera, A. T., Mikić, B. B.**, Exploiting heat transfer instabilities. Resonant heat transfer enhancement, Int. J. Heat Mass Transfer, Vol. 29, No. 8, pp. 1127-1138, 1986.

8. **Durst, F., Founti, M., Obi, S.**, Experimental and computational investigation of the two-dimensional channel flow over two fences in tandem, ASME J. Heat Transfer, Vol. 110, pp. 48-54. 1988.

9. **Trollheden, S., Sundén, B.**, Numerical prediction of flow and heat transfer in a parallel duct with sreamwise periodic variation of cross- sectional area, Proc. 5 Int. Conf. on Numerical Methods in Laminar and Turbulent Flow, Montreal, Canada, Vol.5, Part 2, pp. 1515-1528, 1987.

10. **Sundén, B., Trollheden, S.**, Periodic laminar flow and heat transfer in a corrugated two-dimensional channel, Int. Comm. Heat Mass Transfer, Vol. 16, pp. 215-225, 1989.

11. **Hunter, J. C., Collins, M., W.**, Holographic interferometry and digital fringe processing, J. Phys. D: Appl. Phys., Vol. 20, pp. 683-691, 1987.

12. **Fodemski, T. R., Collins, M. W.**, Flow and heat transfer simulations for two- and three-dimensional smooth and ribbed channels, Proc. 2 UK National Conf. on Heat Transfer, Vol. 1, pp. 845-860, 1988.

13. **Herman, C. V., Mayinger, F.**, Experimental investigation of heat transfer in laminar forced convection flow in a grooved channel, Proc. 9 Int. Heat Transfer Conf., Jerusalem, Israel, pp. 387-392, 1990.

14. **Mayinger, F., Panknin, W.**, Holography in heat and mass transfer, Proc. 5 Int. Heat Transfer Conf., Tokyo, Japan, pp. 28-43, 1974.

15. **Vest, C. M.**, Holographic interferometry, John Wiley & Sons, New York, 1979.

16. **Herman, C. V., Mewes, D., Mayinger, F.**, Optical techniques in transport phenomena, to be published in Advances in Transport Processes VIII, A. S. Mujumdar, R. A. Mashelkar, eds., 1990.

17. **Hauf, W., Grigull, U.**, Optical methods in heat transfer, in Advances in Heat Transfer, Vol. 6, Academic Press Inc., New York, 1970.

18. **Sterr, S.**, Diplomarbeit, Lehrstuhl A für Thermodynamik, TU München, 1989.